MANY FACES OF NON-EQUILIBRIUM: ANOMALOUS TRANSPORT PHENOMENA IN DRIVEN PERIODIC SYSTEMS

P. Hänggi

Institute of Physics, University of Augsburg, 86135 Augsburg, Germany
and
Nanosystems Initiative Munich, 80799 München, Germany

J. Łuczka, J. Spiechowicz

Institute of Physics, University of Silesia, 41-500 Chorzów, Poland

We consider a generic system operating under non-equilibrium conditions. Explicitly, we consider an inertial classical Brownian particle dwelling a periodic structure with a spatially broken reflection symmetry. The particle is coupled to a bath at the temperature T and is driven by an unbiased time-periodic force. In the asymptotic long-time regime, the particle operates as a Brownian motor exhibiting finite directed transport although no net biasing force acts on the system. Here, we review and interpret in further detail our own recent research on the peculiar transport behaviour for this set-up. The main focus is put on those different emerging Brownian diffusion anomalies. Particularly, within the transient, time-dependent domain, the particle is able to exhibit anomalous diffusive motion which eventually crosses over into normal diffusion only in the asymptotic long-time limit. In the latter limit, this normal diffusion coefficient may even show a non-monotonic temperature dependence, meaning that it is not monotonically increasing with increasing temperature, but may exhibit instead an extended, intermediate minimum before growing again with increasing temperature.

1. Introduction

The theory for equilibrium systems is far from being complete. For example, the stationary state of a system strongly interacting with a surrounding thermostat is generally not available [1]. Despite this incompleteness for equilibrium set-ups, there are laws in nature which allow us to predict their

reaction to an external perturbation. A celebrated example constitutes the Le Chatelier–Braun principle [2–5] which, loosely speaking, states that if a system in equilibrium is subjected to a perturbation, a reaction will occur so that the equilibrium will be shifted towards a new one, counteracting this change. This principle may be regarded as a precursor of a linear response theory [6, 7] which nowadays is a common tool for predicting the properties of a system in equilibrium perturbed by an external stimuli. An archetypal example is the Sutherland–Einstein relation [8–10], saying that for such set-ups, the diffusion coefficient is an increasing function of temperature.

Despite many years of active research, our current understanding of non-equilibrium physics fundamentals is still incomplete, undoubtedly far beyond what we known for equilibrium systems. Yet, much progress has been achieved over the last decades in modelling certain aspects of such systems such as stochastic resonance [11], noise assisted transport far from equilibrium [12, 13], absolute negative mobility [14–19], anomalous diffusion [20–22] or various recent fluctuation theorems [23, 24], to name only a few. Here, we aim to demonstrate that non-equlibrium conditions allow for a rich complexity which is not present in a system at thermal equilibrium. The reason behind it is that equilibrium is ruled by various Thermodynamic Laws and symmetries such as, for example, *detailed balance*, which generally loose their validity if taken out of equilibrium. For this purpose, we survey recent research on peculiar transport behaviour occurring in temporally driven periodic system with the particular emphasis put on diffusion anomalies. We rely on the Langevin equation description for the non-linear Brownian motion which, as we shall demonstrate, can also be successfully applied to non-equilibrium systems. It can be derived from a corresponding microscopic Hamiltonian description complemented by fundamentals of equilibrium statistical physics imposed on the thermostat [6]. The system of interest may look simple at first glance; however, the emerging underlying inertial dynamics is exceptionally rich upon observing that the driven Brownian motion is governed by several parameters which in turn yield a complex dynamics.

2. Generic model of an inertial Brownian motor

In this work, we consider a classical Brownian motor [13]. It is typically modelled as an inertial particle of mass M which moves in a spatially periodic potential $U(x)$ which breaks reflection symmetry and, additionally, is driven by an unbiased time-periodic force $A\cos(\Omega t)$ of amplitude A and angular frequency Ω. The system is coupled to thermostat of temperature T. The corresponding Langevin equation reads

$$M\ddot{x} + \Gamma\dot{x} = -U'(x) + A\cos(\Omega t) + \sqrt{2\Gamma k_{\mathrm{B}}T}\,\xi(t)\,, \tag{1}$$

where the dot and the prime denote differentiation with respect to time t and the Brownian particle coordinate x, respectively. The parameter Γ stands for the kinetic friction coefficient and k_{B} denotes the Boltzmann constant. The interaction with thermostat is modelled by δ-correlated, Gaussian white noise $\xi(t)$ of vanishing mean and unit intensity, *i.e.*

$$\langle \xi(t) \rangle = 0 , \qquad \langle \xi(t)\xi(s) \rangle = \delta(t - s) . \tag{2}$$

The spatially periodic potential $U(x)$ is assumed to be reflection non-symmetric, *i.e.* of a ratchet-type [13, 25]. As an example, we choose a double-sine form of period $2\pi L$ and barrier height $2\Delta U$; explicitly,

$$U(x) = -\Delta U \left[\sin\left(\frac{x}{L}\right) + \frac{1}{4} \sin\left(2\frac{x}{L} + \varphi - \frac{\pi}{2}\right) \right] . \tag{3}$$

Before we start the analysis of this set-up, we need to transform the above equation of motion in its dimensionless form. Towards this aim, we introduce dimensionless distance and time variables for the system under consideration [26, 27]; *i.e.* we set

$$\hat{x} = \frac{x}{L} , \qquad \hat{t} = \frac{t}{\varkappa_0} , \qquad \varkappa_0 = \frac{\Gamma L^2}{\Delta U} , \tag{4}$$

so that the dimensionless form of the Langevin dynamics (1) reads

$$m\ddot{\hat{x}} + \dot{\hat{x}} = -\hat{U}'(\hat{x}) + a\cos\left(\omega\hat{t}\right) + \sqrt{2Q}\hat{\xi}\left(\hat{t}\right) . \tag{5}$$

Here, the dimensionless potential $\hat{U}(\hat{x}) = U(x)/\Delta U = U(L\hat{x})/\Delta U = \hat{U}(\hat{x} + 2\pi)$ possesses the period 2π and half of the barrier height is $\Delta\hat{U} = 1$. The remaining parameters are scaled as: $m = M/(\Gamma\varkappa_0)$, $a = (L/\Delta U)A$, $\omega = \varkappa_0\Omega$. The rescaled thermal noise reads $\hat{\xi}(\hat{t}) = (L/\Delta U)\xi(t) = (L/\Delta U)\xi(\varkappa_0\hat{t})$ and assumes the same statistical properties as $\xi(t)$, namely $\langle\hat{\xi}(\hat{t})\rangle = 0$ and $\langle\hat{\xi}(\hat{t})\hat{\xi}(\hat{s})\rangle = \delta(\hat{t} - \hat{s})$. The dimensionless noise intensity $Q = k_{\mathrm{B}}T/\Delta U$ is the ratio of thermal and half of the activation energy the particle needs to overcome the non-rescaled potential barrier. In order to simplify the notation further, we shall omit the $\wedge$-notation in Eq. (5).

The above proposed scaling procedure is not unique as one is free to define other characteristic time scales of the system described by Eq. (1); namely,

$$\varkappa_0 = \frac{\Gamma L^2}{\Delta U} , \qquad \varkappa_1 = \frac{M}{\Gamma} , \qquad \varkappa_2^2 = \frac{ML^2}{\Delta U} , \qquad \varkappa_3 = \frac{2\pi}{\Omega} . \tag{6}$$

Note that only three of them are independent because $\varkappa_0\varkappa_1 = \varkappa_2^2$. Here, we use as the unit of time $\varkappa_0$, see in Eq. (4) above. This corresponds to the

characteristic time scale for an overdamped particle to move from the maximum of the potential $U(x)$ to its minimum. It can be extracted from the equation $\Gamma \dot{x} = -U'(x)$. The scale $\varkappa_1$ denotes a relaxation time of the velocity $v = \dot{x}$ of the free Brownian particle (*i.e.* for the choice $U(x) = A = 0$) which is obtained from the relation $M\ddot{x} + \Gamma \dot{x} = 0$. Note that here, the dimensionless mass emerges as $m = \varkappa_1/\varkappa_0$; *i.e.* it equals the ratio of these two characteristic time scales. The quantity $\varkappa_2$ is a characteristic time scale for the conservative system (when $\Gamma = A = 0$) and follows from the equation $M\ddot{x} = -U'(x)$. It is related to the period of particle linearized oscillations within one potential well. The remaining third time scale $\varkappa_3$ is the period of the external time-periodic force. Thermal fluctuations are modelled here approximately as white noise. In real systems, however, it is never strictly zero but physically typically much smaller than the other time scales.

The limit $\Gamma \to \infty$, implying that $m \to 0$, presents an overdamped thermal rocking ratchet dynamics, whose adiabatic and alike its non-adiabatic driving regimes have been previously thoroughly studied in Refs. [28, 29] in both, its stochastic dynamics at finite temperatures and as well in its deterministic limit [28, 30]. Remarkably, this overdamped deterministic regime is already rather complex, exhibiting, for example, locking regimes which follow a devil's staircase behaviour [29, 30].

Potential (3) has originally been derived for the asymmetric superconducting quantum interference device (SQUID) which is composed of a loop with three capacitively and resistively shunted Josephson junctions [31–35]. The particle coordinate x and velocity v correspond to the Josephson phase and the voltage drop across the device, respectively. The particle mass stands for the capacitance of the SQUID, the friction coefficient translates to the reciprocal of the SQUID resistance. The time-periodic force corresponds to the modulated external current. The asymmetry parameter φ of potential (3) can be controlled by an external magnetic flux which pierces across the device.

From a mathematical point of view, Eq. (5) is a second order differential equation additionally complemented by a random force. At first glance, it seems simple for undertaking a study. However, note that even the phase space of the noiseless autonomous system modelled by Eq. (5) is already three-dimensional $\{x, y = \dot{x}, z = \omega t\}$; therefore, being minimal for it to display a chaotic dynamics [36]. Moreover, the underlying parameter space $\{m, a, \omega, Q, \varphi\}$ is five-dimensional, thus exhibiting a rich and correspondingly highly complex behaviour. The probability density $P(x, v, t)$ for the particle coordinate x and its velocity v obeys a Fokker–Planck equation corresponding to the Langevin equation (5) [37]. It is a parabolic partial differential equation with a time-periodic drift coefficient in phase space of position and velocity. Combining it with a non-linear periodic potential $U(x)$

together with a five-dimensional parameter space implies that corresponding analytic time-dependent solutions become in practice unattainable and we are thus forced to use advanced numerical resources. Details of the latter are elaborated in Ref. [38]. However, for large dimensionless times $(t \gg 1)$, the probability density $P(x, v, t)$ approaches the asymptotic periodic probability distribution $P_{\mathrm{as}}(x, v, t) = P_{\mathrm{as}}(x, v, t + \mathsf{T})$ with the periodicity $\mathsf{T} = 2\pi/\omega$ of the time-periodic driving $a\cos(\omega t)$ [39–41].

3. Transient regime: anomalous diffusion

The diffusion behaviour of the particle dynamics and the spread of its trajectories is conventionally characterized by the mean-square deviation (variance) of the particle position $x(t)$ [20], namely,

$$\sigma_x^2(t) = \left\langle [x(t) - \langle x(t) \rangle]^2 \right\rangle = \left\langle x^2(t) \right\rangle - \langle x(t) \rangle^2 \,, \tag{7}$$

where the averaging $\langle \cdot \rangle$ is over all realizations of thermal fluctuations as well as over the initial conditions for the position $x(0)$ and the velocity $\dot{x}(0)$. The latter is necessary because in the deterministic limit of vanishing thermal noise intensity $Q \to 0$, the dynamics may possess several coexisting attractors thus being non-ergodic and implying that the corresponding results may be affected by a specific choice of those selected initial conditions [42]. If the coordinate variance grows linearly in evolving time; *i.e.*

$$\sigma_x^2(t) = 2Dt \tag{8}$$

we refer to diffusion as *normal* and the parameter D is termed the diffusion coefficient. Any deviation from this strict linearity qualifies as a process exhibiting anomalous diffusion [20, 43–45]. For anomalous diffusion, the variance assumes an increasing function of elapsing time, growing either according to a sub-diffusive or a superdiffusive power law [20]

$$\sigma_x^2(t) \sim t^\alpha \,. \tag{9}$$

Normal diffusion is observed for $\alpha = 1$. The case of $0 < \alpha < 1$ refers to subdiffusion, while the case of $\alpha > 1$ is classified as superdiffusion. It becomes appropriate for the following discussion to consider a time-dependent "diffusion coefficient" $D(t)$, defined by the relation [42]

$$D(t) = \frac{\sigma_x^2(t)}{2t} \,. \tag{10}$$

If the behaviour is as in (9), then $D(t) \sim t^{\alpha-1}$ and

— $D(t)$ is time-decreasing for subdiffusion,

— $D(t)$ is constant for normal diffusion,

— $D(t)$ is time-increasing for superdiffusion.

We stress that only in the asymptotic long-time regime with the exponent α approaching unity, we find a properly defined, finite diffusion coefficient D, *i.e.*

$$D = \lim_{t\to\infty} D(t) < \infty \,. \tag{11}$$

If the diffusion process is anomalous, then $D(t)$ either converges to zero (for subdiffusion) or diverges to infinity (for superdiffusion) when $t \to \infty$.

In panels (a) and (b) of Fig. 1, we depict time evolution of the diffusion coefficient $D(t)$ and the coordinate mean square deviation $\sigma_x^2(t)$, respectively, for two values of the noise intensity $Q \propto T$. At first glance, it is difficult to identify whether in fact anomalous diffusion takes place by just inspecting the behaviour for $\sigma_x^2(t)$. In distinct contrast, from inspecting instead the behaviour for $D(t)$, it becomes more facile to differentiate between the two anomalous types of diffusion: superdiffusion occurs in the interval where $D(t)$ increases, while the case of decreasing $D(t)$ corresponds to subdiffusion. For an invariant $D(t)$, normal diffusion takes place. In panel (a), the evolution of $D(t)$ can be divided into the three following time-intervals: an early behaviour of superdiffusion $(0, \tau_1)$, an intermediate temporal interval (τ_1, τ_2) where subdiffusion emerges over several decades and an asymptotic long-time regime $t > \tau_2$ where normal diffusion occurs. The crossover times τ_1 and τ_2 separating these domains can be controlled by the temperature or noise intensity. For a lower temperature (*i.e.* $Q = 0.00016$, see the grey/red curve in panel (a)), the lifetime of superdiffusion is extremely long. In fact, it tends to infinity when $Q \to 0$ (the deterministic case). For $Q = 0.00016$, the superdiffusion regime extends to $\tau_1 \approx 3.2 \times 10^6$. It is difficult to numerically determine τ_2 due to limited stability of the utilized algorithm, leading to uncontrolled propagation of roundoff- and truncation-errors. However, if we adopt an extrapolation from other cases, then the time τ_2 is at least of the order of $10^{11} \sim 10^{13}$. For higher temperature ($Q = 0.0007$, the black/blue curve in panel (a)), the lifetime τ_1 is shorter and it tends to zero when the temperature tends to infinity. For $Q = 0.0007$, the superdiffusion lifetime is at $\tau_1 \approx 3.2 \times 10^3$ and for subdiffusion it is at $\tau_2 \approx 10^8$. For higher temperatures, the dynamics is initially superdiffusive and approaches a normal diffusion behaviour without exhibiting an intermediate subdiffusion time-interval. It is important to note that generally the anomalous diffusion behaviour is only of a transient nature and eventually it always tends to normal diffusion in the asymptotic long-time limit.
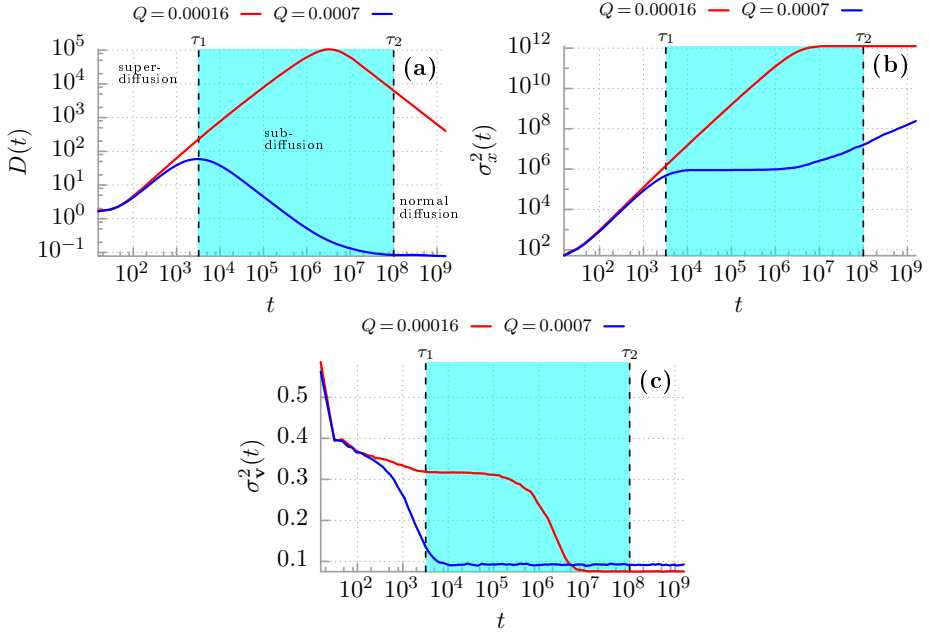
Fig. 1. (Colour on-line) Transient anomalous diffusion of an inertial Brownian particle moving in a periodic potential and driven by a unbiased time-periodic force. In panel (a), we present the diffusion coefficient $D(t)$ as defined in Eq. (10). Panel (b) depicts time evolution of the coordinate variance $\sigma_x^2(t)$. In panel (c), the period averaged velocity variance $\sigma_v^2(t)$ is shown. Two cases of thermal noise intensity Q proportional to temperature are presented (grey/red and black/blue line). The region corresponding to the subdiffusive behaviour is for the intensity set at $Q = 0.0007$ (region in light grey/cyan colour). The remaining parameters are chosen as: $m = 6$, $a = 1.899$, $\omega = 0.403$. The rescaled potential is $U(x) = -\sin(x) - (1/4)\sin(2x)$, which corresponds to $\varphi = \pi/2$. These panels are reproduced from Ref. [51].

4. Asymptotic normal long-time diffusion: Non-monotonic temperature dependence

In the standard Sutherland–Einstein relation [8, 9] valid for systems at thermal equilibrium, the diffusion coefficient D is a monotonically increasing linear function of temperature T, *i.e.*

$$D = \mu k_{\mathrm{B}} T, \qquad (12)$$

where μ is a mobility coefficient. This is in accordance with our intuition because when temperature grows, then thermal fluctuations become larger and, in consequence, fluctuations of the particle position also increase. However, for some parameter regimes of our non-equilibrium set-up, we observe an

atypical, non-monotonic temperature dependence for the emerging asymp-
totic normal diffusion constant D [46]. An example is presented with Fig. 2.
At low temperatures Q, the diffusion coefficient increases with increasing Q
until it reaches a local maximum at $Q \approx 2 \times 10^{-5}$ (*cf.* dark grey/red line).
Then it *decreases* towards a minimum at $Q \approx 5 \times 10^{-3}$ before turning over
into a monotonically growing function of Q; finally, at sufficiently large val-
ues of Q, the diffusion coefficient D becomes precisely proportional to Q; *i.e.*
to the temperature T of the ambient thermal bath. This high-temperature
behaviour, however, is not depicted in Fig. 1. The decrease of the diffusion
constant with increasing temperature $Q \propto T$ is truly counter-intuitive, be-
ing in clear contrast with the Sutherland–Einstein relation (12) as well as
with other known relations such as for example Vogel–Fulcher-like laws [47]
or an Arrhenius-type behaviour for the diffusion of a Brownian particle in
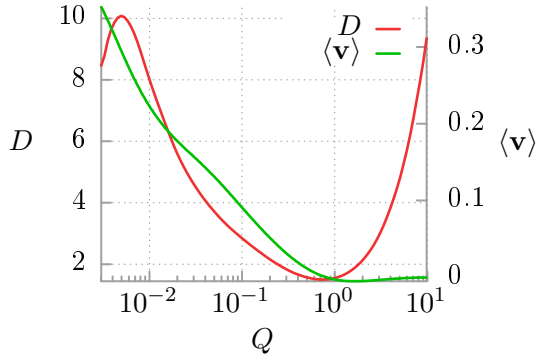periodic potentials [48–50].

Fig. 2. (Colour on-line) The dependence of the asymptotic diffusion coefficient D
(left-hand side ordinate) and the directed velocity $\langle \boldsymbol{v} \rangle$ (right-hand side ordinate,
see Eq. (16)) *versus* the noise intensity Q, the latter being proportional to the
temperature T of the bath. The chosen parameters are: $m = 6$, $a = 1.899$,
$\omega = 0.403$, $\varphi = \pi/2$. The panel is reproduced from Ref. [46].

5. Averaged velocity of the Brownian motor

In order to explain the above two anomalous transport phenomena, one
needs first to carefully examine the deterministic structure of the phase
space $\{x, v\}$ of all coordinates and velocities of the Brownian motor. For
the presented parameter regime, *cf.* Figs. 1 and 2, the noiseless system with
$Q = 0$ is non-chaotic with three coexisting attractors $\{v_+, v_0, v_-\}$ in the
velocity subspace $\{v\}$. These attractors correspond to running solutions
with $v_+ \approx 0.4$ and $v_- \approx -0.4$, and the locked solution $v_0 \approx 0$. There are
three classes of trajectories corresponding to these three states: $x_+(t) \sim 0.4t$,

$x_-(t) \sim -0.4t$ and $x_0(t) \sim 0$. The basins of attraction for these attractors is shown in Fig. 3. The grey/red and dark grey/blue sets consist of all initial conditions $\{x(0), v(0)\}$ evolving into the running states with either positive $v_+ \approx 0.4$ and negative $v_- \approx -0.4$ velocity, respectively. The light grey/green colour regimes mark the locked states with $v_0 \approx 0$.
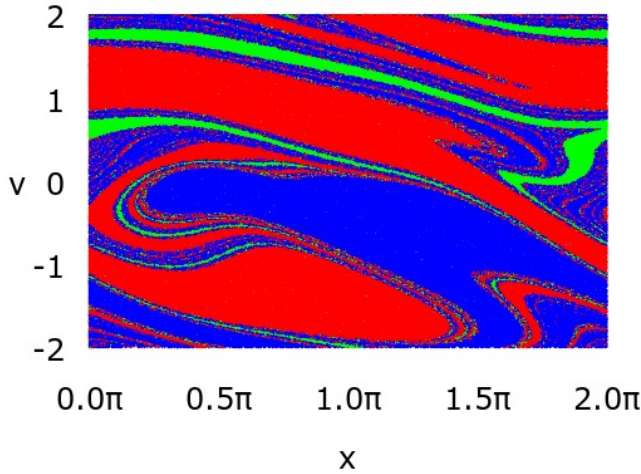

Fig. 3. (Colour on-line) Basins of attraction for the asymptotic long-time particle velocity $\boldsymbol{v}(t)$. The grey/red and dark grey/blue coloured sets consist of all initial conditions $\{x(0), \dot{x}(0)\}$ eventually evolving to the running states with the positive $v_+ \approx 0.4$ and negative $v_- \approx -0.4$ velocity, respectively. The light grey/green colour marks the set of locked states $v_0 \approx 0$. Parameters are: $m = 6$, $a = 1.899$, $\omega = 0.403$, $\varphi = \pi/2$. For this particular regime the deterministic system (5) with $Q = 0$ is non-chaotic. Panel reproduced from [42].

When the noise intensity is non-vanishing, then thermal fluctuations induce a stochastic dynamics which destabilizes those attractors and leads to random transitions between its coexisting basins of attraction. This situation is analogous to an escape dynamics from metastable wells in multistable equilibrium systems [50]. Such transitions between the running and/or locked states may generate the transient anomalous diffusion documented with the previous sections. Since we are interested not only in the asymptotic state but also in the full time dynamics, it is useful to consider the averaged velocity over the realizations and here additionally also over the temporal driving period of the Brownian motor, in presence of thermal noise; *i.e.*

$$\langle \boldsymbol{v}(t) \rangle = \frac{\omega}{2\pi} \int_{t}^{t+2\pi/\omega} ds \, \langle \dot{x}(s) \rangle \qquad (13)$$

and its variance

$$\sigma_{\boldsymbol{v}}^2(t) = \left\langle \boldsymbol{v}^2(t) \right\rangle - \left\langle \boldsymbol{v}(t) \right\rangle^2 . \tag{14}$$

In the asymptotic long-time limit, these so double-averaged quantities become time-independent, while the solely noise-averaged quantities alone assume a time-periodic function of the asymptotic time-periodic (with period T) phase-space probability $P_{\mathrm{as}}(x, v, t) = P_{\mathrm{as}}(x, v, t + \mathsf{T})$. Put differently, in the asymptotic long-time limit, the mean velocity $\langle \dot{x}(t) \rangle$ takes the form of a Fourier series over all possible higher harmonics of the driving force [11, 39, 41]

$$\lim_{t \gg 1} \langle \dot{x}(t) \rangle = \langle \boldsymbol{v} \rangle + v_\omega(t) + v_{2\omega}(t) + \dots , \tag{15}$$

where $\langle \boldsymbol{v} \rangle$ is the time-independent (dc) component, while $v_{n\omega}(t)$ denote time-periodic higher harmonic functions of zero average over the fundamental period $\mathsf{T} = 2\pi/\omega$ of the driving. The averaged directed velocity $\langle \boldsymbol{v} \rangle$ can also be obtained from Eq. (13), namely,

$$\langle \boldsymbol{v} \rangle = \lim_{t \gg 1} \langle \boldsymbol{v}(t) \rangle . \tag{16}$$

Due to the presence of the external driving, the Brownian motor is taken far away from thermal equilibrium and a time-dependent non-equilibrium state is reached in the asymptotic long-time regime. Since all forces in the right-hand side of Eq. (5) are non-biased, a necessary condition for the occurrence of directed transport $\langle \boldsymbol{v} \rangle \neq 0$ is the breaking of the reflection symmetry of the potential $U(x)$ [13, 25], *cf.* the left panel of Fig. 4.
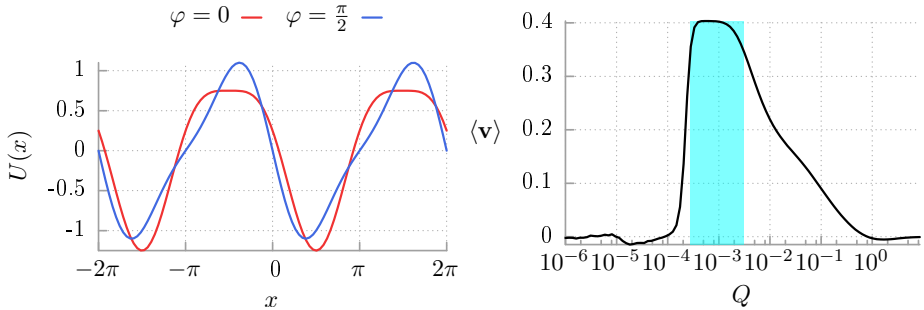

Fig. 4. (Colour on-line) Left panel: The potential given by Eq. (3) depicted in the symmetric case $\varphi = 0$ and its ratchet form for the asymmetry parameter $\varphi = \pi/2$. Right panel: The asymptotic long-time averaged directed velocity $\langle \boldsymbol{v} \rangle$ *versus* the noise intensity Q, being proportional to temperature T of the ambient bath. Parameters are: $m = 6$, $a = 1.899$, $\omega = 0.403$, $\varphi = \pi/2$. Right panel is reproduced from [52].

In the right panel of Fig. 4, we plot the directed velocity $\langle v \rangle$ as a function of temperature $Q \propto T$. For vanishing intensity $Q \to 0$ of thermal fluctuations, the directed velocity $\langle v \rangle \to 0$, which is in agreement with the probability distribution $P(v(t))$ of the individual asymptotic long-time period averaged motor velocity for the deterministic variant of system (5) with $Q = 0$. It is so because of the weighted average over the two running attractors $v_- = 0.4$ and $v_+ = 0.4$ as well as the locked state $v_0 = 0$ yields a vanishing $\langle v \rangle = 0$. For slightly higher temperature, we observe small fluctuations around the deterministic value $\langle v \rangle = 0$. A further growth of temperature causes a notable enhancement of the particle velocity $\langle v \rangle \approx 0.4$. We marked this region with the grey/cyan colour. In this regime, for the deterministic counterpart of the system, there is no directed transport of the motor, however thermal fluctuations induce it. The reason for this behaviour is concealed in thermally activated jumps in the phase space of the non-equilibrium dynamics.

6. Mechanism responsible for anomalous transport

Let us now explain the mechanisms which are at the origin for the above presented transport anomalies:

(i) *Superdiffusion* [42]. In the deterministic case of $Q = 0$, there are three attractors in the velocity subspace and there are three classes of trajectories associate with them: $x_+(t) \sim 0.4t$, $x_-(t) \sim -0.4t$ and $x_0(t) \sim 0$. The overall mean value of the particle position is negligibly small $\langle x(t) \rangle \approx 0$, meaning that also $\langle v \rangle \approx 0$. Moreover, this fact implies that the mean-square deviation $\langle \Delta x^2(t) \rangle = \langle x^2(t) \rangle - \langle x(t) \rangle^2 \approx \langle x^2(t) \rangle \sim t^2$. As a consequence, superdifusive transport takes place which in fact is ballistic diffusion in this deterministic case. This superdiffusive regime is persistent only if $Q \to 0$. For $Q > 0$, thermal noise induces repeated stochastic transitions among the deterministic solutions $x_+(t)$, $x_-(t)$ and $x_0(t)$ which in turn allow for the occurrence of finite directed Brownian motor transport $\langle v \rangle \neq 0$ if the reflection symmetry of the system is broken, *cf.* Fig. 4. In particular, as temperature grows progressively, more transitions from the trajectories $x_-(t)$ and $x_0(t)$ to the solution $x_+(t) \sim 0.4t$ are observed. There occurs even an intensity interval where almost all particles travel according to $x_+(t) \sim 0.4t$ as then $\langle v \rangle \approx 0.4$, *cf.* grey/cyan colour regime in Fig. 4. The relaxation time of the velocity $\langle v(t) \rangle$ to its asymptotic long-time value $\langle v \rangle$ is the same as the lifetime τ_1 for superdiffusion. If the intensity of thermal fluctuations increases, the frequency of thermally activated transitions between the deterministic solutions grows greater and, therefore, the lifetime for superdiffusion decreases.

(ii) *Subdiffusion* [51, 52]. For the noisy system $Q \neq 0$, the directed transport velocity $\langle v \rangle \neq 0$ and the probability for the particle to be in the positive running state $v_+ \approx 0.4$ grow, whereas the corresponding quantity to stay in the negative running state $v_+ \approx -0.4$ as well as in the locked state $v_0 \approx 0$ decreases. Consequently, the spread of trajectories is smaller and the subdiffusion is developed. It means that once the particles enter the state v_+, they move almost coherently. This argument is supported by the panel (c) of Fig. 1, where the velocity fluctuations are significantly reduced within the time-interval for subdiffusion. These small, but still finite fluctuations are responsible for the ultraslow subdiffusion where the observed scaling index α in Eq. (9) is tiny but nonzero $\alpha \ll 1$ [51]. In the time-interval $\tau_1 < t < \tau_2$ the probability for the particle to be in the state v_+ is extremely close to unity, meaning that almost all particle trajectories are localized in this regime. Finally, for sufficiently long times $t > \tau_2$, random dynamics induced by thermal fluctuations again activate jumps between the coexisting trajectories, thus eventually leading to normal diffusion.

(iii) *Non-monotonic temperature dependence of the diffusion coefficient* [46]. Let us focus on two exemplary temperatures $Q_1 < Q_2$, *e.g.* $Q_1 = 10^{-2}$ and $Q_2 = 1$ in Fig. 2, in order to explain the mechanism responsible for non-monotonic temperature dependence of the diffusion coefficient. Here, we observe that $D(Q_1) > D(Q_2)$. For the lower temperature $Q_1 = 10^{-2}$, the averaged directed velocity is $\langle v \rangle \approx 0.25 > 0$, whereas for larger $Q_2 = 1$, the velocity $\langle v \rangle \approx 0$, *i.e.* $\langle v \rangle(Q_1) > \langle v \rangle(Q_2) \approx 0$. The latter observation means that for the lower temperature, the deterministic structure of the three attractors $\{v_+, v_0, v_-\}$ is still present and plays an important role in controlling the diffusive properties of the system. In particular, because then $\langle v \rangle > 0$, the majority of trajectories is travelling with the positive velocity v_+, nevertheless, a still significant fraction of them follows the locked solution v_0 and alike also the negative running solution v_-. The probability distribution for the particle velocity can approximately be represented by a sum of three Gaussians of different mean values, representing the corresponding deterministic solution $\{v_+, v_0, v_-\}$. This causes a large overall spread among the particles and, as a consequence, also for the corresponding diffusion coefficient. For larger temperature $\langle v \rangle \approx 0$, the deterministic structure of attractors ceases to be of relevance. In such a case, the probability distribution of the particle velocity can be approximated by a single Gaussian with zero mean. Now, the spread between the trajectories is only due to variance of the latter probability distribution which is significantly smaller as compared to the case with lower tem-

peratures. Consequently, the diffusion coefficient is reduced. For even larger growing temperature $Q > Q_2$, the diffusion coefficient behaves in a standard way and increases with increasing temperature. This corroborates the finding that for higher temperature, the variance of the Gaussian probability distribution for the particle velocity becomes larger.

7. Summary

We have shown that for an inertial non-linear Brownian motor dynamics modelled by an equation which at first glance may appear simple, *i.e.* for a one-dimensional Newton equation driven by random forces and external driving, the resulting diffusive dynamics manifests an exceptionally rich spectrum of physical phenomena, including counter-intuitive anomalous transport behaviours. The main reason responsible for these features is that the system operates far away from thermal equilibrium. Even the asymptotic long-time state is manifest non-equilibrium and its analytical form is far from being accessible analytically. Therefore, the only applicable scheme for the analysis of this archetype set-up is via numerical simulations. The latter can explain the physics of the occurring phenomena, but only on a qualitative level. A remaining open question then is to what extent this simple, stylized set-up with its already complex behaviour can still serve as a trustworthy paradigm for describing those anomalous transport features occurring in more realistic complex systems possessing many more degrees of freedom.

REFERENCES

[1] P. Talkner, P. Hänggi, «Colloquium: Statistical mechanics and thermodynamics at strong coupling: quantum and classical», `arXiv:1911.11660 [cond-mat.stat-mech]`.

[2] A.L. Chatelier, «Sur un eńonceǵeńeŕal des lois de l'eq́uilibre chimique», *Comptes. Rendus.* **99**, 786 (1884).

[3] F. Braun, «Einige Bemerkungen zu dem vorstehenden Aufsatze», *Z. Physik. Chem.* **1**, 269 (1887).

[4] F. Braun, «Ueber einen allgemeinen qualitativen Satz für Zustandsänderungen nebst einigen sich anschliessenden Bemerkungen, insbesondere über nicht eindeutige Systeme», *Ann. Phys.* **33**, 337 (1888).

[5] L.D. Landau, E.M. Lifshitz, «Statistical physics. Part I», *Butterworth-Heinemann*, 1980.

[6] R. Kubo, «The fluctuation–dissipation theorem», *Rep. Prog. Phys.* **29**, 255 (1966).

[7] U.M.B. Marconi, A. Puglisi, L. Rondoni, A. Vulpiani, «Fluctuation–dissipation: Response theory in statistical physics», *Phys. Rep.* **461**, 111 (2008).

[8] W. Sutherland, «LXXV. A dynamical theory of diffusion for non-electrolytes and the molecular mass of albumin», *Phil. Mag.* **9**, 781 (1905).

[9] A. Einstein, «Über die von der molekularkinetischen Theorie der Wärme geforderte Bewegung von in ruhenden Flüssigkeiten suspendierten Teilchen», *Ann. Phys. (Leipzig)* **17**, 549 (1905).

[10] P. Hänggi, F. Marchesoni, «Introduction: 100 years of Brownian motion», *Chaos* **15**, 026101 (2005).

[11] L. Gammaitoni, P. Hänggi, P. Jung, F. Marchesoni, «Stochastic resonance», *Rev. Mod. Phys.* **70**, 223 (1998).

[12] J. Kula, M. Kostur, J. Łuczka, «Brownian transport controlled by dichotomic and thermal fluctuations», *Chem. Phys.* **235**, 27 (1998).

[13] P. Hänggi, F. Marchesoni, «Artificial Brownian motors: Controlling transport on the nanoscale», *Rev. Mod. Phys.* **81**, 387 (2009).

[14] R. Eichhorn, P. Reimann, P. Hänggi, «Brownian motion exhibiting absolute negative mobility», *Phys. Rev. Lett.* **88**, 190601 (2002).

[15] Ł. Machura *et al.*, «Absolute negative mobility induced by thermal equilibrium fluctuations», *Phys. Rev. Lett.* **98**, 040601 (2007).

[16] J. Nagel *et al.*, «Observation of negative absolute resistance in a Josephson junction», *Phys. Rev. Lett.* **100**, 217001 (2008).

[17] J. Spiechowicz, J. Łuczka, P. Hänggi, «Absolute negative mobility induced by white Poissonian noise», *J. Stat. Mech.* **2013**, P02044 (2013).

[18] J. Spiechowicz, P. Hänggi, J. Łuczka, «Brownian motors in the microscale domain: Enhancement of efficiency by noise», *Phys. Rev. E* **90**, 032104 (2014).

[19] A. Slapik, J. Łuczka, P. Hänggi, J. Spiechowicz, «Tunable mass separation via negative mobility», *Phys. Rev. Lett.* **122**, 070602 (2019).

[20] R. Metzler, J.-H. Jeon, A. Cherstvy, E. Barkai, «Anomalous diffusion models and their properties: non-stationarity, non-ergodicity, and ageing at the centenary of single particle tracking», *Phys. Chem. Chem. Phys.* **16**, 24128 (2014).

[21] J. Łuczka, R. Rudnicki, P. Hänggi, «The diffusion in the quantum Smoluchowski equation», *Physica A* **351**, 60 (2005).

[22] J. Spiechowicz, P. Hänggi, J. Łuczka, «Coexistence of absolute negative mobility and anomalous diffusion», *New J. Phys.* **21**, 083029 (2019).

[23] C. Jarzynski, «Equalities and inequalities: Irreversibility and the second law of thermodynamics at the nanoscale», *Annu. Rev. Condens. Matter Phys.* **2**, 329 (2011).

[24] M. Campisi, P. Hänggi, P. Talkner, «Colloquium: Quantum fluctuation relations: Foundations and applications», *Rev. Mod. Phys.* **83**, 771 (2011).

[25] S. Denisov, S. Flach, P. Hänggi, «Tunable transport with broken space-time symmetries», *Phys. Rep.* **538**, 77 (2014).

[26] J. Spiechowicz, J. Łuczka, «Diffusion anomalies in ac-driven Brownian ratchets», *Phys. Rev. E* **91**, 062104 (2015). See also article addendum at `arXiv:1506.00105 [cond-mat.stat-mech]`.

[27] A. Słapik, J. Łuczka, J. Spiechowicz, «Negative mobility of a Brownian particle: Strong damping regime», *Commun. Nonlinear Sci. Numer. Simulat.* **55**, 316 (2018).

[28] R. Bartussek, P. Hänggi, J.G. Kissner, «Periodically rocked thermal ratchets», *Europhys. Lett.* **28**, 459 (1994).

[29] P. Hänggi, R. Bartussek, «Brownian rectifiers: How to convert Brownian motion into directed transport», in: J. Parisi, S.C. Müller, W. Zimmermann (Eds.) «Nonlinear physics of complex systems. Lecture Notes in Physics, Vol. 476», *Springer Berlin Heidelberg, 1996*, pp. 294–308.

[30] D. Cubero *et al.*, «Overdamped deterministic ratchets driven by multifrequency forces», *Acta Phys. Pol. B* **37**, 1467 (2006).

[31] R.L. Kautz, «Noise, chaos, and the Josephson voltage standard», *Rep. Prog. Phys.* **59**, 935 (1996).

[32] I. Zapata, R. Bartussek, F. Sols, P. Hänggi, «Voltage rectification by a SQUID ratchet», *Phys. Rev. Lett.* **77**, 2292 (1996).

[33] J. Spiechowicz, P. Hänggi, J. Łuczka, «Josephson junction ratchet: The impact of finite capacitances», *Phys. Rev. B* **90**, 054520 (2014).

[34] A. Sterk, R. Kleiner, D. Koelle, «Three-junction SQUID rocking ratchet», *Phys. Rev. Lett.* **95**, 177006 (2005).

[35] J. Spiechowicz, J. Łuczka, «Josephson phase diffusion in the superconducting quantum interference device ratchet», *Chaos* **25**, 053110 (2015).

[36] S. Strogatz, «Nonlinear dynamics and chaos: With applications to physics, biology, chemistry and engineering», *Westview Press*, 2015.

[37] H. Risken, «Fokker–Planck equation», in: «The Fokker–Planck equation: Methods of solution and applications», *Springer, Berlin, Heidelberg, 1996*.

[38] J. Spiechowicz, M. Kostur, Ł. Machura, «GPU accelerated Monte Carlo simulation of Brownian motors dynamics with CUDA», *Comput. Phys. Commun.* **191**, 140 (2015).

[39] P. Jung, P. Hänggi, «Resonantly driven Brownian motion: Basic concepts and exact results», *Phys. Rev. A* **41**, 2977 (1990).

[40] P. Jung, P. Hänggi, «Amplification of small signals via stochastic resonance», *Phys. Rev. A* **44**, 8032 (1991).

[41] P. Jung, «Periodically driven stochastic systems», *Phys. Rep.* **234**, 175 (1993).

[42] J. Spiechowicz, J. Łuczka, P. Hänggi, «Transient anomalous diffusion in periodic systems: ergodicity, symmetry breaking and velocity relaxation», *Sci. Rep.* **6**, 30948 (2016).

[43] F. Hofling, T. Franosch, «Anomalous transport in the crowded world of biological cells», *Rep. Prog. Phys.* **76**, 046602 (2013).

[44] Y. Meroz, I.M. Sokolov, «A toolbox for determining subdiffusive mechanisms», *Phys. Rep.* **573**, 1 (2015).

[45] V. Zaburdaev, S. Denisov, J. Klafter, «Lévy walks», *Rev. Mod. Phys.* **87**, 483 (2015).

[46] J. Spiechowicz, M. Kostur, J. Łuczka, «Brownian ratchets: How stronger thermal noise can reduce diffusion», *Chaos* **27**, 023111 (2017).

[47] I. Goychuk, V.O. Kharchenko, «Anomalous features of diffusion in corrugated potentials with spatial correlations: Faster than normal, and other surprises», *Phys. Rev. Lett.* **113**, 100601 (2014).

[48] S. Lifson, J.L. Jackson, «On the self-diffusion of ions in a polyelectrolyte solution», *J. Chem. Phys.* **36**, 2410 (1962).

[49] R. Festa, E. d'Agliano Galleani, «Diffusion coefficient for a Brownian particle in a periodic field of force», *Physica A* **90**, 229 (1978).

[50] P. Hänggi, P. Talkner, M. Borkovec, «Reaction-rate theory: fifty years after Kramers», *Rev. Mod. Phys.* **62**, 251 (1990), see Sect. VII therein.

[51] J. Spiechowicz, J. Łuczka, «Subdiffusion via dynamical localization induced by thermal equilibrium fluctuations», *Sci. Rep.* **7**, 16451 (2017).

[52] J. Spiechowicz, J. Łuczka, «SQUID ratchet: Statistics of transitions in dynamical localization», *Chaos* **29**, 013105 (2019).